Pure Appl. Geophys. 172 (2015), 2411–2420

DOI 10.1007/s00024-015-1060-7

Pure and Applied Geophysics

Ground-Motion Simulation in the Lower Tagus Valley Basin

J. F. Borges,[1] M. Bezzeghoud,[1] B. Caldeira,[1] and João Carvalho[2]

Abstract—Throughout history, the Lower Tagus Valley (LTV) region has been shaken by several earthquakes, including some with moderate to large magnitudes and with sources located inside the basin, for example the 1344 (M6.0) and 1909 (M6.0) earthquakes. Previous simulations (Bezzeghoud *et al*. Natural Hazard 69: 1229–1245, 2011) have revealed strong amplification of the amplitude waves in the region, because of the effect of the low-velocity sediments that fill the basin. The model used in those simulations was updated in this work by including new high-resolution geophysical and geotechnical data available for the area (seismic reflection, aeromagnetic, gravimetric, deep wells, standard penetration tests, and geological data). To contribute to improved assessment of seismic hazard in the LTV, we simulated propagation of seismic waves produced by moderate earthquakes in a 3D heterogeneous medium by using elastic finite-difference wave propagation code. The method, successfully used by Grandin *et al*. (Geophys J Int 171: 1144–1161, 2007), involves evaluation of the seismic potential of known faults in the area studied and three-dimensional seismic ground motion modelling by use of finite difference methods. On the basis of this methodology, we calculated the ground motion for the April 23, 1909, Benavente (Portugal) earthquake ($Mw = 6.0$) in dense grid points, then computed the synthetic isoseismic map of the area by use of appropriate relationships between seismic intensity (MMI) and peak ground velocity (PGV). The synthetic results, in contrast with available macroseismic and instrumental data, enable validation of the source models proposed for the area, identification of the sources of historical earthquakes, and could also indicate which areas are more exposed to seismic ground motion.

1. Introduction

To the best of our knowledge, the strongest motion predictions in earthquake hazard analysis for the LTV basin have been made by use of empirical methods based on attenuation–distance curves for peak ground acceleration (PGA) and peak ground velocity (PGV) as a function of magnitude, fault distance, and ground amplification conditions. Two recent studies focussing on the LTV reflect this trend: Carvalho *et al*. (2008) used a stochastic approach to simulate and compare ground motion shaking in the city of Lisbon and its surroundings by using onshore and offshore sources; Vilanova and Fonseca (2007) adopted a classic probabilistic seismic hazard approach (PSA) to estimate seismic hazard in Portugal. However, none of this work takes into account the kinematic and dynamic propagation of rupture, or wave propagation in complex and irregular sedimentary basins. Significant amplification of ground motion during major earthquakes, the so-called site effect (or basin effect), is known to occur in highly complex basins, for example the LTV. This effect has been verified by simulations (Grandin *et al*. 2007a, b and Bezzeghoud *et al*. 2011) for the Lower Tagus Valley and other Meso-Cenozoic basins of the mainland of Portugal. More recently, Bezzeghoud *et al*. (2011) showed that use of a stratified one-dimensional (1D) model is completely inappropriate for estimation of peak ground velocity (PGV) and for waveform modelling in South-western Iberia because the crustal structure varies dramatically along the ray paths, with large-scale heterogeneities of low or high velocities. In recent years, because of 3D structure model improvement and the development of numerical and computational capability, different studies have successfully achieved strong ground-motion synthesis for a range of frequencies up to 1.0 Hz (Hartzell *et al*. 2006; Grandin *et al*. 2007a) and simulations of broadband strong motion by combining a low-frequency waveform full-wave equation with high-frequency stochastic seismograms (hybrid models) (Hartzell *et al*. 2002).

[1] Departamento de Física and Instituto de Ciências da Terra, Escola de Ciências e Tecnologia, Universidade de Évora, Rua Romão Ramalho, 59, 7002-554 Évora, Portugal. E-mail: jborges@uevora.pt

[2] Laboratório Nacional de Energia e Geologia, Lisboa, Portugal.

In this work we concentrate our analysis on ground motion modelling by using an extended source located inside the Lower Tagus Basin to generate synthetic waveforms with wave propagation code based on the finite-difference method. Finally, we compare intensities obtained from peak ground velocities estimated from the synthetic waveforms with observed intensities for the 1909 Benavente earthquake, in an attempt to identify its source, which remains a question of debate (Cabral *et al*. 2003).

2. *Tectonic Setting of the Lower Tagus Valley Basin*

The LTV basin, located in central Portugal and which includes the city of Lisbon with a population of 600,000 habitants, is oriented in a NE direction and covers an approximate area of 3200 km^2. Figure 1 shows the location and seismicity of the study area. The Basin is a complex tectonic depression in which Cenozoic sediments have been deposited and preserved on a thick Mesozoic sequence of up to 2000 m. Cenozoic geological units comprises Paleogene to Pliocene sediments, Pleistocene fluvial terraces, and a thick (up to 70 m) Upper Pleistocene to Holocene alluvial cover (Cabral *et al*. 2003).

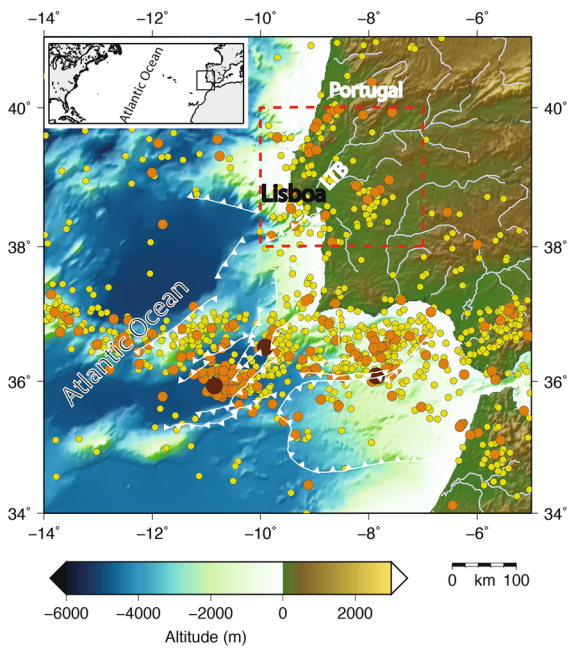

Figure 1
Instrumental seismicity for the period 1961–2014 (IPMA data base). The bathymetric lines from ETOPO2 (US Department of Commerce, NOAA/NGDC, 2001) and the major active faults (adapted from Zitellini *et al*. 2001) in the southwestern Iberian margin are presented. *LTV* Lower Tagus Valley

Some of the major fault zones that control the evolution of the LTCB are hidden, because of the presence of the sedimentary layer (Cabral *et al*. 2003, 2004; Carvalho et al. 2006, 2014); geophysical methods are, thus, of fundamental importance in their recognition. The seismic reflection method, combined with well data, has been used for many decades (usually in association with the oil industry) to study the stratigraphy and tectonic evolution of sedimentary basins, including the Lower Tagus/Lusitanian Basin. However, only a limited part of the basin (the south-western part, covering less than 10 % of the total area) was sampled by seismic reflection profiles.

For large areas, for which seismic and drilling data are unavailable or too expensive to be practical, the potential-field (magnetic and gravimetric) method can be very useful for characterisation of sedimentary basins and for obtaining depth-to-basement estimates. This was the situation for the Lower Tagus Valley basin used in this work. We have produced a top of the basement map for the LTV region and adjacent areas by using:

1 seismic reflection and well data (Carvalho *et al*. 2014) for the areas where these data were available; and
2 potential-field data for the areas with no seismic coverage.

Figure 1 shows the location of the study area, situated in the central Portuguese mainland and the seismicity of the area.

3. *Seismicity of the Lower Tagus Valley Basin*

Several significant earthquakes have occurred in the LTV. On the basis of reports of these earthquakes, the most important are believed to have originated in the SW Iberia margin (Borges *et al*. 2001; Bezzeghoud *et al*. 2011). Such destructive earthquakes were most likely to have been generated by N–S to NNE–SSW trend offshore structures located SW of

the Portuguese coastline (Zitellini *et al*. 1999, 2001; Grandin *et al*. 2007b; Carvalho *et al*. 2012; Terrinha *et al*. 2003). The study area has also suffered the effects of moderate events originating from local sources which caused much destruction and significant damage; the maximum intensity was IX in Benavente, Vila Franca de Xira, and Lisbon, and resulted in the loss of many lives (Moreira 1985; Henriques *et al*. 1988) (Fig. 2).

Many authors have suggested that the local historical events that affected the LTV Basin and the city of Lisbon where the 1344, 1531, and 1909 (Mw = 6.0) earthquakes. Of these three events, only the 1909 earthquake occurred in the period when instrumental monitoring was possible, so well-constrained moment magnitude determination (6.0, according to Teves-Costa *et al*. 1999; Stich *et al*. 2005) and relatively well constrained epicentre determination has been possible by use of macroseismic data. After the 1909 earthquake, the seismic activity in the area has been rather weak with only two earthquakes exceeding magnitude 5 in this region: the September 23 and 25 1914 (M = 5.3) earthquakes.

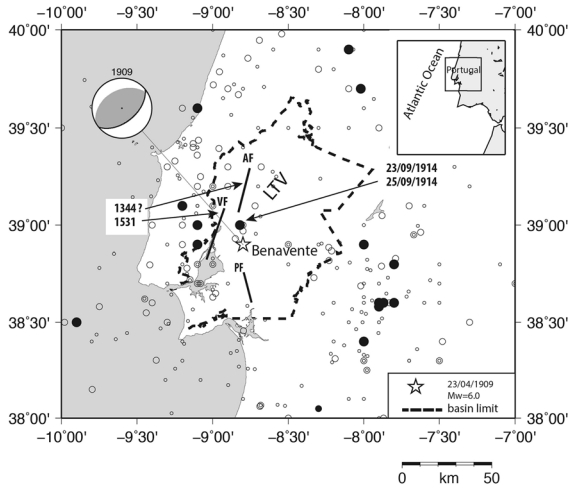

Figure 2
Instrumental seismicity for the period 1961–2014 for events with magnitude $M > 1$ (*open circles*, IPMA data base). The 1909 Benavente epicentre (*star*) and the most relevant earthquakes after the 1909 main shock (Mw = 6.0) are also represented (*black dots*). The *dashed line* shows the limit of the Lower Tagus Valley (LTV) basin. Main faults inside LTV: *AF* Azambuja Fault, probably related to the 1344 event; *VF* Vila Franca de Xira Fault, probably related to the 1531 earthquake; *PF* Porto Alto Fault.; focal mechanism of the 1909 earthquake (Stich *et al*. 2005) (*black line* represents the fault plan used in this work)

After these two events, seismic activity has been limited to the occurrence of micro events with maximum felt intensity of III. For example, the number of events that occurred in the period from 1990 to 2014 (the period in which modernization of the national seismographic network began) with magnitude between 2 and 3 was 45, and only five events of magnitude ranging between 3 and 4 occurred in that period. Nevertheless, not a single strong motion record was produced in all the instrumental period.

With regard to the 1344 earthquake, although several authors believe the epicentral area was in the LTV region (Justo and Salwa 1998) doubts about its location remain, because this earthquake initiated a huge tsunami that could not have been caused by elastic deformation inside the Tagus Estuary, as demonstrated by numerical modelling (Miranda *et al*. 2012).

In addition, the geometry, topography, and geological conditions of the LTV Cenozoic Basin and the Lusitanian Mesozoic Basin (located to the west) are important in local amplification and site effects that mask the relationship between the location of historical events (based on seismic intensity studies) and the sources of the earthquakes (Grandin *et al*. 2007a).

4. Velocity model

We propose a crustal velocity model in the region lying between latitudes 38.5°N and 40°N and between longitudes 7.5°W and 9.5°W. The model includes the seismogenic zones of the LTV. The model takes into account the properties of the crustal structure with the objective of reproducing ground motion at low and intermediate frequencies ($f < 1.2$ Hz). Overall, the resulting velocity structure is marked mainly by the presence of the LTV Basin—less consolidated sediments with relatively low wave seismic velocity—and the Lusitanian Neogene basin.

In this model, the crust is considered stratified and is made of a superposition of a finite number of layers of different depth and thickness. Only the depth of each interface between layers must be specified at given points; a Delaunay triangulation can then be used to fill the spaces between these points (Watson

1982). A layer can thus taper off and reach zero thickness.

The system of classification of continental crust layers uses nine different layers with distinct physical identified properties. These overlie the upper mantle, which is modelled as a half-space, with a uniform P-velocity of 8.1 km s^{-1} and a *Vp*/*Vs* ratio of 1.74 to deduce S-wave velocities from P-wave velocities (Grandin *et al*. 2007a). Densities were set based on experimental measurements of density for a set of crustal rocks.

The velocity model we propose (Fig. 3) is contained in a more extensive model of SW Iberia (SWIBMOD2006 model) that was proposed by Grandin *et al*. (2007a) as the basis for simulation of large earthquakes generated in the SW margin of the Iberian Peninsula. The model proposed (LISMOT) in this study incorporates a grid of data much denser than that of the previous model. Some of the data (those of the best quality) were obtained by reinterpretation of oil-industry seismic profiles and are restricted to relatively small area of the SW part of the basin. A sparse network of profiles obtained from magnetic and gravity survey inversion constrained by seismic, deep wells and geological outcrop data (average spacing approximately 40 km) cover the remaining part of the basin.

5. *Ground Motion Simulation of the 1909 Benavente Earthquake*

We chose to use the 1909 Benavente event ($Mw = 6.0$) to test the ability of our model to simulate credible synthetic ground motion because it is one of the most documented in the study area (Bensaude 1910; Teves-Costa and Batlló 2010). This event is also the only one on the Portuguese mainland for which intensity data points with small epicentral distances systematically covering the basin are available.

To model the propagation of seismic waves in a 3D medium, we used the code E3D, which is explicit 2-D/3-D elastic finite-difference wave propagation code (Larsen and Schultz 1995). The medium is assumed to be elastic and isotropic, and the systems of the equations of motion and constitutive laws are

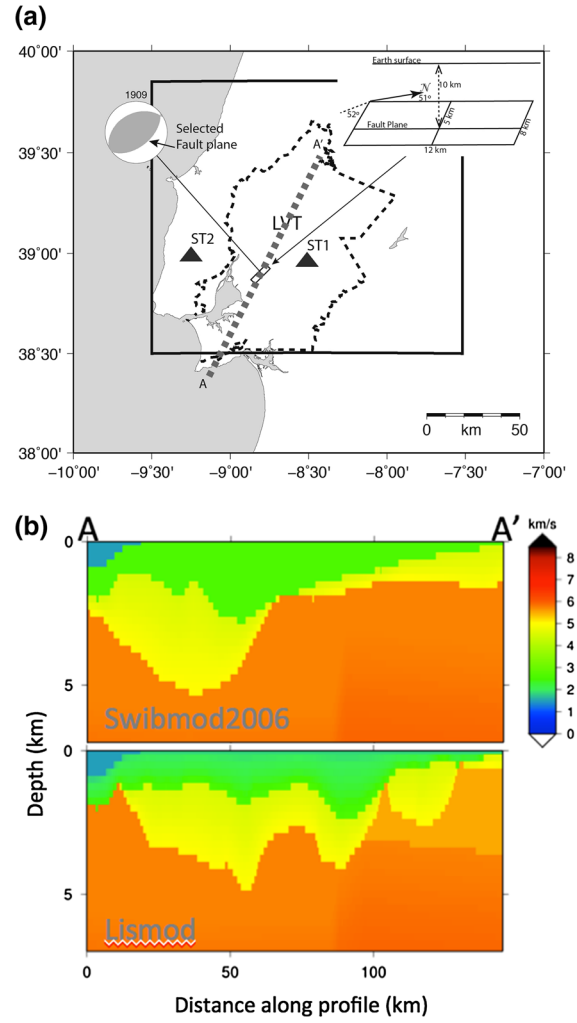

Figure 3
a Location of the cross-section between 9.3°W, 38.4°N and 8.4°W, 39.5°N and ST1 and ST2 stations. The *top right corner* shows the fault model with the main data used for the simulations. The *black rectangle* shows the simulation area. **b** Cross-section of the SWIBMOD model (Grandin *et al*. 2007a) and the LISMOD model proposed in this study. The *yellow layers* correspond to indurated sediments (Mesozoic and Palaeogene units), and the *green layers* correspond to recent, poorly consolidated sediments (Cenozoic sediments)

solved numerically on a grid staggered in both space and time (Madariaga 1976), considering uniform grid spacing. To ensure low numerical dispersion, the shortest wavelength in the model must be sampled at five grid-points per wavelength (Levander 1988).

More details of the method and computational issues related to the finite-difference scheme are presented elsewhere Grandin *et al*. (2007a). This

numerical method has been successfully applied to 3D structure models by a large number of authors for generation of synthetic seismograms. It has also been applied in Portugal (Grandin *et al*. 2007a, b; Bezzeghoud *et al*. 2011) to the Western part of Iberia for an exceptionally large region, 400 × 400 km, with grid spacing between 1 and 0.5 km (yielding a maximum frequency of 0.6 Hz) and for earthquakes with magnitudes $5.3 < Mw < 8.5$.

For a source similar to that of the 1909 Benavente earthquake ($Mw = 6.0$), the finiteness of the fault dimensions and of the duration of rupture cannot be ignored. The ratio between the estimated size (~10 km) and the range of epicentral distances used in this work (10–150 km) is not compatible with a point source model. Following the source implementation scheme of E3D, we model this extended source by superimposing a large number of point sources over a rectangular fault plane (the number of points and their position depend on the discretisation adopted and on the area and dip of the fault plane). The ratio between the estimated size (~10 km) and the range of epicentral distances used in this work (10–150 km) is not compatible with a point source model (Table 1).

We use the solution of Stich et al. (2005), the reverse mechanism solution (depth = 10 km strike = 51°, dip = 52°, and rake = 83°), and a total moment of 1.1×10^{18} Nm ($Mw = 6.0$), a value similar to that obtained by Teves-Costa *et al*. (1999) from the horizontal displacement spectra of S-waves. We also chose a rectangular fault with a length of 12.5 km, a width of 8 km, and a hypocentre depth of 10 km, located 5 km in the downdip direction from the fault trace, where the rupture nucleates (details of the characteristics of the fault for grid spacing of 0.5 km and 0.25 km are shown in Fig. 3a and listed in Table 2).

Because of the absence of physical or geological evidence we arbitrarily adopted the plane with azimuth 51°N. We tested the conjugated plan and we arrived at similar results in synthetic waveforms and peak ground velocities. This is not surprising, because the fault plans have a similar direction.

As the elementary source time function for rupture on each subfault we chose to use a source time function proposed by Beresnev and Atkinson (1997) (based on the "omega-squared" spectrum Brune signal (Brune 1970) (Fig. 4a). Assuming circular rupture with a velocity of 2.5 km/s, a grid spacing of 0.25 km, and a rise time τ of 0.1 s, we can conclude that the rupture initiates on a sub-fault when the previous sub-fault has reached approximately 25 per cent of the total displacement. We also assume a uniform slip distribution over the whole fault plane.

Table 1

Fault and source parameters used for computation of synthetic seismograms and isoseismal maps of the 1909 Benavente earthquake

Lat (°)	Long (°)	Nucleation depth/downdip (km)	Length (km)	Width (km)	Fault azimuth (°)	Focal mechanism			Seismic moment (Nm)
						Strike (°)	Dip (°)	Rake (°)	
38.90 N	–	8.80 W 1.1×10^{18}	10/5	12	8.0	51	51	52	83

The focal mechanism, seismic moment, and coordinates are those proposed by Stich *et al*. (2005)

Table 2

Main values used in the E3D simulations

dh (km)	Dimensions (km)			Grid size (number of nodes)	Time step (s)	Maximum frequency (Hz)
	East (km)	North	Depth			
0.5	225	175	70	451 × 351 × 241	0.030	0.625
0.25	225	175	70	901 × 701 × 281	0.015	1.25

dh = grid spacing in all directions

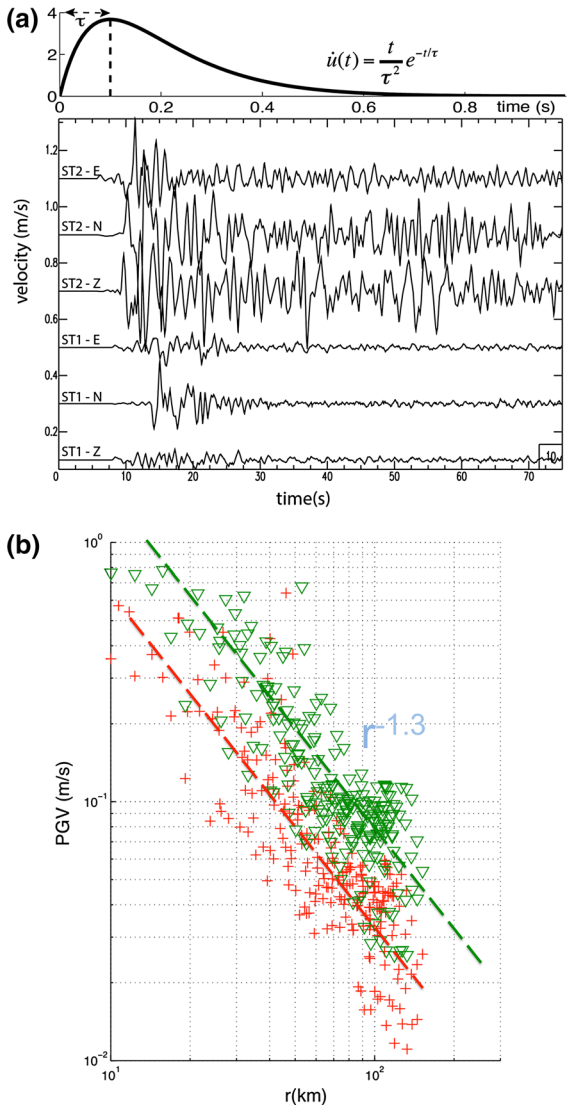

Figure 4

a *Top*: source time function used for simulations with 0.25-km grid spacing (source time function proposed by Beresnev and Atkinson 1997); τ is the rise time of the elementary source time function (0.1 s for grid spacing of 250 m and 0.2 s for grid spacing of 500 m. *Bottom*: synthetic seismograms (velocity) calculated for the ST1 and ST2 stations (locations shown in Fig. 3a) (*E*, *N*, and *Z* correspond to the E–W, N–S, and vertical components of synthetic seismograms). **b** Fall-off of PGV as a function of distance for two simulations with different grid spacing (0.5 km in *red* and 0.25 km in *green*)

In this study, synthetic seismograms should, consequently, be limited to frequencies smaller than the highest frequency f_{max}, which is given by:

$$f_{max} = c_{min}/5 \times dh, \quad (1)$$

where c_{min} is the minimum velocity in the grid and dh is the grid spacing. Considering a grid spacing of $dh = 0.25$ km and a minimum velocity of shear waves of 1.5 km s^{-1}, we arrive at a maximum frequency f_{max} of 1.2 Hz for the synthetic seismograms. For a finite source, the rupture velocity is fixed at 2.5 km s^{-1}, and we also consider a time step of $dt = 0.015$ s to satisfy the Courant condition. The calculation was run for more than 5000 time steps, which corresponds to a time window of 75 s, including all the most important phases, particularly the most energetic, for example the S-waves and the surface waves. Figure 3a, b show SW–NE seismic cross-sections (A–A') of the SWIBMOD model (Grandin *et al.* 2007a) and of the LISMOD model proposed in this study, both crossing the epicentre.

The synthetic seismograms were calculated for a dense surface grid of points separated by 10 km and a bandpass filter between 0.05 and 1.2 Hz, using a two-pass four-pole Butterworth filter. The horizontal PGV for all the points of the surface grid were acquired from these seismograms.

We tested the effect of the directivity on the synthetic waveforms and PGV, and concluded there was no significant effect on the results for the different scenarios considered. Figure 4a shows an example of two synthetic seismograms calculated for two different geologically sites: ST1, located inside the LTV basin, and ST2, located outside the basin (the locations are given in Fig. 3a). We conclude there is a strong amplification effect inside the LTV basin, where the S-wave and a surface wave dispersion trend can be clearly identified (Fig. 4a).

Figure 4b shows the relationship between the horizontal PGV and distance to the epicentre for two different grid spacings (0.5 and 0.25 km) in the simulation. Because we are interested in comparing synthetic and observed intensities, we converted the PGV to intensities.

Seismic intensities can be estimated from peak ground motion parameter (PGP) (displacement, velocity or acceleration) by use of the empirical relationship given by the equation:

$$\mathrm{MMI} = a\log(\mathrm{PGP}) + b. \quad (2)$$

The value of a mostly affects geometric attenuation of intensity; b is a constant. Wald *et al.* (1999)

Table 3

Attenuation relationships deduced from the best-fit between Intensities (observed and predicted) and the distance of global data and of data from simulation sites inside and outside the LTV basin area

Intensities	Global		Internal		External	
	a	b	a	b	a	b
Observed	−0.79	6.31	−1.10	6.65	−0.41	6.01
Synthetic ($dh = 0.5$)	−1.19	4.73	−8.26	6.27	−0.63	4.10
Synthetic ($dh = 0.25$)	−0.52	6.90	−0.62	7.51	−0.31	6.70

and Wu *et al.* (2003) suggested that for high intensities (>VII), PGV correlates better with modified Mercalli intensity (MMI) scale than the peak ground displacement (PGD) or the peak ground PGA. Grandin *et al.* (2007b) determined for the SW Iberian Margin (which includes the LTV Basin) that values a and b for Eq. (2) were equal to 3.5 and 10.5, respectively (the PGV is expressed in m/s).

6. Discussion and conclusions

We modelled seismic ground motion of the 1909 Benavente earthquake in the LTV area by using an extended source located inside the basin. We used a 3D model of the basin and wave propagation code based on the finite difference method (Madariaga 1976; Larsen and Schultz 1995). We concluded the following:

1. The amplitude of the seismic waves experiences significant amplification in the basin. This amplification increases with the depth of the basement (as already demonstrated by Bezzeghoud *et al.* 2011). In Fig. 4a it is possible to identify strong amplification in the synthetic seismogram of the ST1 station located inside the basin (mainly in the horizontal components of the seismogram) compared with the ST2 station located outside the LTV basin. There is, in addition, enlargement of the coda of the seismogram caused by reverberation of the seismic waves inside the basin.
2. The PGV values obtained by simulations depend on the maximum frequency of the synthetic waveforms, which requires a study of attenuation conducted on the basis of seismic data collected in the basin. However, this is a difficult task because of reduced seismicity and the absence of a seismographic network located inside the Basin. The difference between PGV (and intensity) for grid spacing of 500 and 250 m (Figs. 4a, 6b) can be justified by the vertical under-sampling of the basin that can occur for grid spacing of 500 m, which has the effect of attenuation of the velocity contrasts between the sediment and the substrate. Because it is known that amplification is greater the higher the velocity contrast between the substrate and the Cenozoic cover, smaller PGV and intensity are expected for a lower resolution mesh.
3. From analysis of the dependence of seismic Intensities (synthetic and observed intensities) on the logarithm of the distance (Fig. 6a; Table 3) we concluded that this relationship is linear and decreasing. This behaviour reflects the effect of

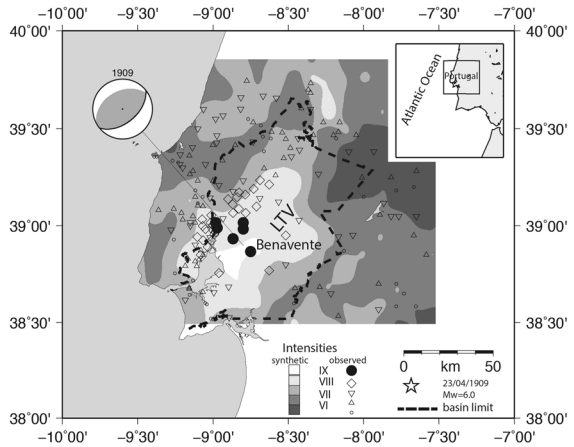

Figure 5
Comparison of simulated synthetic intensities for a grid spacing of 0.25 m obtained in this study and observed intensities from Teves-Costa and Batlló (2010)

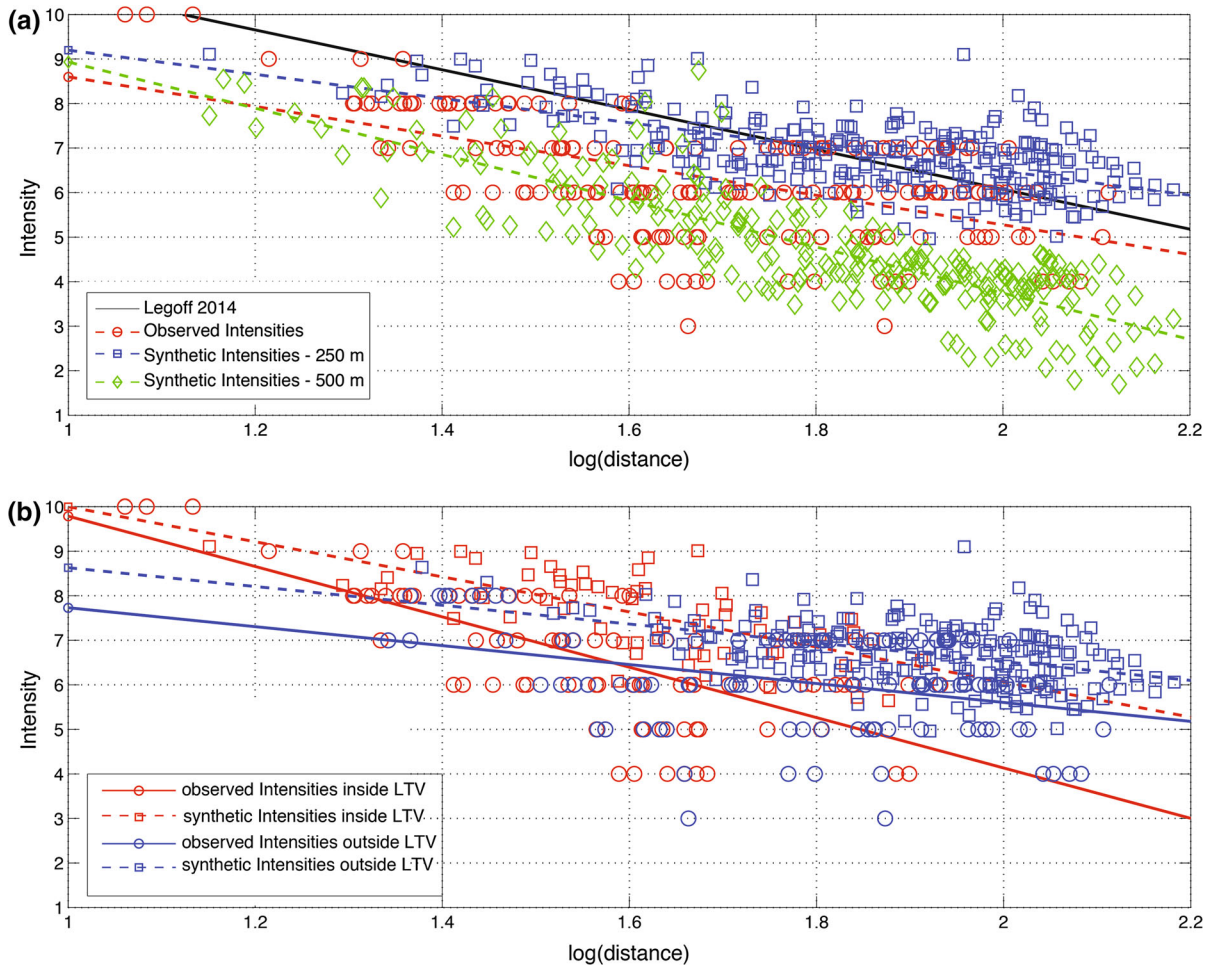

Figure 6

Relationship between seismic Intensity (synthetic and observed) and the logarithm of the distance best fit as obtained by use of linear regression: **a** for all simulated points inside the simulation domain, for both resolutions (250 and 500 m), for the observed data (Teves-Costa and Batlló 2010), and in comparison with the Le Goff *et al*. (2014) attenuation law obtained for the Portugal mainland area; **b** solely for simulations of 0.25 km grid spacing and for points inside and outside the basin

the geometric attenuation and constitutes an attenuation law (Le Goff *et al*. 2014).

By separating points inside the basin from points outside the basin we arrive at dual behaviour of the attenuation. In fact, attenuation is more intense within the basin than outside. This behaviour is common to both types of intensity, as shown in Fig. 6b and Table 3.

4. The synthetic isoseismal lines (Fig. 5) have an elliptical shape with a direction coincident with the axis of the basin. This is not a source effect related to the directivity of the rupture or radiation pattern, as we conclude from the different simulations, and must be related with the geological structure of the basin. We did not confirm the strong stretching in the EW direction on the isoseismal map of the Benavente earthquake as shown by Teves-Costa and Batlló (2010).
5. The decrease in intensity with distance, represented in the Fig. 6b, is stronger within the basin than in the external part of the basin. This behaviour, found both in the observed and synthetic data, is expected, because of structure of the basin and the strong interdependence of sediment thickness and the amplification of seismic waves.

6. Seismic intensities of IX are well reproduced by this simulation but intensities of VIII and VII in the simulation cover a larger area than for the observed intensities. One possible explanation is inadequate source location and/or characteristics.

   Several factors may affect ground motion; we believe, however, on the basis of the simulations we ran, that uncertainty in the seismic source parameters is not the most important factor. Indeed, the geological structure generates strong distortions in soil movements (site effects or basin effect, and topographic effects), and the maximum frequency of 1.2 Hz obtained in this work does not account for all known propagation effects. Recent studies in the LTV basin (Borges *et al*. 2015) reveals strong amplification for frequencies between 1 and 2 Hz as a result of the amplification effect produced by alluvial deposits of the river and its tributaries, with S-wave velocities and a thickness that are not considered in the simulations.
7. Future work will consider other possible earthquake sources and improvement of the 3D velocity model, including the effect of attenuation

Acknowledgments

This work was developed with the support of the Fundação para a Ciência e Tecnologia (FCT/MCTES, Portugal) through the projects SISMOD/LISMOT (PTDC/CTE- GIN/64228/2006), ATESTA (PTDC/CTE-GIX/099548/2008), NEFITAG (PTDC/CTE-GIX/102245/2008), LTV-SourceMod4PSHA (PTDC/CTE-GIX/101852/2008), QuakeLoc (PTDC/GEO-FIQ/3522/2012), and PEst-OE/CTE/UI0078/2011.

References

Bensaude, A. (1910). *Le Tremblement de Terre de la Vallee du Tage du 23 Avril 1909 (Note prelim- inaire), Extrait du Bull*. de Ia Soc. Portugaise des Sciences Naturelles – Tome IV – fasc 2–3, Lisbonne, Imprimerie Typ. de Ia Librairie Ferin, Lisbon.

Bezzeghoud, M., Borges, J.F., and Caldeira, B. 2011. *Ground Motion Simulations of the SW Iberia Margin: Rupture Directivity and Earth Structure Effects*. Natural Hazard *69*, 2, 1229–1245.

Beresnev, I. A. and G. M. Atkinson (1997). *Modeling finite-fault radiation from the omega**n spectrum*, Bulletin of the Seismological Society of America *87*, 67–84.

Borges, J. F., Fitas, A. J. S., Bezzeghoud, M. & Teves- Costa, P. (2001). *Seismotectonics of Portugal and its adjacent Atlantic area*. Tectonophysics *337*, 373–387.

Borges, J. F; Silva, H.G.; Torres, R.J.G.; Caldeira, B.; Bezzeghoud, M. Furtado, J. A. and Carvalho, J, 2015. Inversion of ambient seismic noise HVSR to evaluate velocity and structural models of the Lower Tagus Basin, Portugal. submitted to Seismological Research Letters.

Brune J.N., 1970. *Tectonic stress and spectra of seismic shear waves*. J Geophys Res, *75*: 4997–5009

Cabral, J., Moniz, C., Ribeiro, P., Terrinha, P., Matias, L., 2003. *Analysis of seismic reflection data as a tool for the seismotectonic assessment of a low activity intraplate basin—the Lower Tagus Valley (Portugal)*. Journal of Seismology *7*, 431–447.

Cabral, J., Ribeiro, P., Figueiredo, P., Pimentel, N., Martins, A., 2004. *The Azambuja fault: an active structure located in an intraplate basin with significant seismicity (Lower Tagus Valley, Portugal)*. Journal of Seismology, *8*, 347–362.

Carvalho, J., Cabral, J., Gonçalves, R., Torres, L., and Mendes-Victor, L., 2006. *Geophysical methods applied to fault characterization and earthquake potential assessment in the Lower Tagus Valley, Portugal*, Tectonophysics, *418*, 277–297

Carvalho, A., Zonno, G., Franceschina, G., Bilé Serra J. and Campos Costa, A., 2008, *Earthquake shaking scenarios for the metropolitan area of Lisbon*. Soil Dynamics and Earthquake Engineering, *28*, 347–364.

Carvalho, J., Matias, H., Rabeh, T., Menezes, P., Barbosa, V., Dias, R., Carrilho, F., 2012, *Connecting Onshore Structures in the Algarve with the southern Portuguese continental margin: The Carcavai Fault Zone*. Tectonophysics, *570-571*, 151-162, DOI: 10.1016/j.tecto.2012.08.011.

Carvalho, J., Rabeh, T., Dias, R., Dias, R., Pinto, C.C., Oliveira, T., Cunha, T. and Borges, J.F. (2014) *Tectonic and Neotectonic Implications of a New Basement Map of the Lower Tagus Valley, Portugal*. Tectonophysics, *617*, 88–100. http://dx.doi.org/10.1016/j.tecto.2014.01.017.

Grandin, R., Borges, J.F., Bezzeghoud, M., Caldeira, B. and Carrilho, F., 2007a, *Simulations of strong ground motion in SW Iberia for the 1969 February 28 (MS = 8.0) and the 1755 November 1 (M ∼ 8.5) earthquakes – I. Velocity model*, Geophys. J. Int., *171*, 3, 1144–1161. doi:10.1111/j.1365-246X.2007.03570.x.

Grandin, R., Borges, J.F., Bezzeghoud, M., Caldeira, B. And Carrilho, F., 2007b, *Simulations of strong ground motion in SW Iberia for the 1969 February 28 (MS = 8.0) and the 1755 November 1 (M ∼ 8.5) earthquakes – II. Strong ground motion simulations*, Geophys. J. Int., *171*, 2, 807–822, November 2007.doi:10.1111/j.1365-246X.2007.0357.x

Hartzell, S., Leeds, A., Frankel, A., Williams, R.A., Odum, J., Stephenson, W., and Silva, W. (2002). *Simulation of broadband ground motion including nonlinear soil effects for a magnitude 6.5 earthquake on the seattle fault*, Seattle, Washington, BSSA, *92*, 2, 831–853. doi:10.1785/0120010114.

Hartzell, S., Harmsen, S., Williams, R.A., Carver, D., Frankel, A., Choy, G., Liu, P.-C., Jachens, R.C., Brocher, T.M., and Wentworth, C.M. 2006. *Modeling and Validation of a 3D Velocity Structure for the Santa Clara Valley, California, for Seismic-Wave Simulations*, Bull. Seism. Soc. Am., *9*, 5, 1851–1881. doi:10.1785/0120050243

Henriques, M.C., Mouzinho, M.T. and Ferrão, N.M. 1988. Sismicidade de Portugal. O Sismo de 26 de Janeiro de 1531. Comissão para o Catálogo Sísmico Nacional, Lisbon, 100 pp.

Justo JL and Salwa C (1998). *The 1531 Lisbon earthquake*. Bull. Seismol. Soc. America, *88*, 319–328.

Larsen, S.C. & Schultz, C.A., 1995. ELAS3D, 2D/3D Elastic Finite-Difference Wave Propagation Code, Lawrence Livermore National Laboratory, UCRLMA-121792, 18 pp.

Le Goff B., Borges J.F. and Bezzeghoud M. (2014). *Intensity-Distance attenuation laws for the Portugal mainland using intensity data points*, Geophysical Journal International, *199*, 1278–1285. doi:10.1093/gji/ggu317.

Levander, A.R., 1988. *Fourth-order finite-difference P-SV seismograms*, Geophysics, *53*, 1425–1436.

Madariaga R (1976) *Dynamics of an expanding circular fault*. Bull Seismol Soc Am, *66*, 3, 639–666

Miranda, J., Batlló, J., Ferreira, H., Matias, L.M., and Baptista, M.A. (2012). "The 1531 Lisbon earthquake and tsunami". 15 WCEE, Lisboa.

Moreira, V.S., 1985. *Seismotectonics of Portugal and its adjacent area in the Atlantic*, Tectonophysics, 11, 85–96.

Stich, D., Batlló, J., Macià, R., Teves-Costa, P., Morales, J., 2005. *Moment tensor inversion with single-component historical seismograms: the 1909 Benavente (Portugal) and Lambesc (France) earthquakes*. Geophysical Journal International, *162*, 850–858.

Terrinha, P., Pinheiro, L.M., Henriet, J.-P., Matias, L., Ivanov, M.K., Monteiro, J.H., Akhmetzhanov, A., Volkonskaya, A., Cunha, T., Shaskin, P., Rovere, M. and The TTR10 Shipboard Scientific Party (2003). *Tsunamigenic-seismogenic structures, neotectonics, sedimentary processes and slope instability on the southwest Portuguese Margin*. Marine Geology *195*, 55–73.

Teves-Costa P, Borges JF, Rio I, Ribeiro R, Marreiros C (1999) *Source parameters of old earthquakes: semiautomatic digitization of analog records and seismic moment assessment*. Nat Hazarads, *19*, 205–220

Teves-Costa, P., and J. Batlló (2010). *The 23 April 1909 Benavente earthquake (Portugal): Macroseismic field revision*. Journal of Seismology *15*, 1, 59–70; doi:10.1007/s10950-010-9207-6

Vilanova, S., and Joao F. B. D. Fonseca, 2007. *Bulletin of the Seismological Society of America*, Probabilistic Seismic-Hazard Assessment for Portugal, *97*, 5, 1702–1717, doi:10.1785/0120050198

Wald, D.J., Quitoriano, V., Heaton, T.H., Kanamori, H., Scrivner, C.W. and Worden, C.B. (1999). *TriNet "ShakeMaps": rapid generation of instru-mental ground motion and intensity maps for earthquakes in southern California*, Earthq. Spectra, *15*, 537–556.

Watson DF (1982) Automatic contouring of raw data, computers and geosciences. Pergamon Press Ltd., *1*,8, 97–101

Wu, Y.-M., Teng, T.-L., Shin, T.-C. and Hsiao, N.-C. (2003). *Relationship between peak ground acceleration, peak ground velocity, and intensity in Taiwan*, Bull. Seism. Soc. Am., *93*, 386–396.

Zitellini, N., Chierici, F., Sartori, R. and Torelli, L., 1999, *The tectonic source of the 1755 Lisbon earthquake and tsunami*, Annali di Geofisica, *42*, 1, 49-55.

Zitellini N et al., (2001). *Source of the 1755 Lisbon earthquake and tsunami investigated*, EOS Trans. Amer. Geophys. U., *82*, 285.

(Received July 14, 2014, revised February 24, 2015, accepted February 26, 2015, Published online March 12, 2015)